



HAL
open science

Prospective assessment of circulating tumor DNA in patients with metastatic uveal melanoma treated with tebentafusp

Manuel Rodrigues, Toulsie Ramtohol, Aurore Rampanou, José Luis Sandoval, Alexandre Houy, Vincent Servois, Léah Mailly-Giacchetti, Gaelle Pierron, Anne Vincent-Salomon, Nathalie Cassoux, et al.

► **To cite this version:**

Manuel Rodrigues, Toulsie Ramtohol, Aurore Rampanou, José Luis Sandoval, Alexandre Houy, et al.. Prospective assessment of circulating tumor DNA in patients with metastatic uveal melanoma treated with tebentafusp. *Nature Communications*, 2024, 15 (1), <10.1038/s41467-024-53145-0>. <hal-04758281>

HAL Id: hal-04758281

<https://hal.science/hal-04758281v1>

Submitted on 19 Nov 2024

HAL is a multi-disciplinary open access archive for the deposit and dissemination of scientific research documents, whether they are published or not. The documents may come from teaching and research institutions in France or abroad, or from public or private research centers.

L'archive ouverte pluridisciplinaire **HAL**, est destinée au dépôt et à la diffusion de documents scientifiques de niveau recherche, publiés ou non, émanant des établissements d'enseignement et de recherche français ou étrangers, des laboratoires publics ou privés.



Distributed under a Creative Commons CC BY-NC-ND 4.0 - Attribution - Non-commercial use - No Derivative Works - International License

Prospective assessment of circulating tumor DNA in patients with metastatic uveal melanoma treated with tebentafusp

Received: 5 March 2024

Accepted: 30 September 2024

Published online: 14 October 2024

Check for updates

Manuel Rodrigues ^{1,2}, Toulis Ramtohol³, Aurore Rampanou⁴, José Luis Sandoval⁴, Alexandre Houy ², Vincent Servois ³, Léah Mailly-Giacchetti², Gaëlle Pierron ⁵, Anne Vincent-Salomon ⁶, Nathalie Cassoux⁷, Pascale Mariani⁷, Caroline Dutriaux⁸, Marc Pracht⁹, Thomas Ryckewaert¹⁰, Jean-Emmanuel Kurtz¹¹, Sergio Roman-Roman^{2,12}, Sophie Piperno-Neumann¹, François-Clément Bidard ^{1,4,13}, Marc-Henri Stern ² & Shufang Renault ⁴

Tebentafusp, a bispecific immune therapy, is the only drug that demonstrated an overall survival benefit in patients with metastatic uveal melanoma (MUM). Circulating tumor DNA (ctDNA) has emerged as a potential prognostic and predictive marker in the phase 3 IMCgp100-202 trial using multiplex PCR-based next-generation sequencing (NGS). In this study (NCT02866149), ctDNA dynamics were assessed using droplet digital PCR (ddPCR) in 69 MUM patients undergoing tebentafusp treatment. Notably, 61% of patients exhibited detectable ctDNA before treatment initiation, which was associated with shorter overall survival (median 12.9 months *versus* 40.5 months for patients with undetectable ctDNA; $p < 0.001$). Patients manifesting a 90% or greater reduction in ctDNA levels at 12 weeks demonstrated markedly prolonged overall survival (median 21.2 months *versus* 12.9 months; $p = 0.02$). Our findings highlight the potential of ddPCR-based ctDNA monitoring as an economical, pragmatic and informative approach in MUM management, offering valuable insights into treatment response and prognosis.

Uveal melanoma (UM) is the most common primary intraocular tumor in adults affecting ~2-8 individuals per million and per year¹. Metastatic disease eventually develops in approximately 30 to 50% of the patients, mainly in the liver with a median progression-free survival

(PFS) and overall survival (OS) of ~3-4 months and ~10-16 months, respectively². In case of liver metastases, no systemic therapy option had demonstrated an OS benefit until the recent approval of tebentafusp. Tebentafusp is a bispecific protein consisting of an affinity-

¹Department of Medical Oncology, Institut Curie, Paris and Saint Cloud, France. ²Inserm U830, DNA Repair and Uveal Melanoma (D.R.U.M.) team, Institut Curie, PSL Research University, Paris, France. ³Department of Radiology, Institut Curie, PSL Research University, Paris, France. ⁴Circulating Tumor Biomarkers Laboratory, Inserm CIC-BT 1428, Department of Translational Research, Institut Curie, Paris, France. ⁵Somatic Genetic Unit, Department of Genetics, Institut Curie, PSL Research University, Paris, France. ⁶Department of Pathology, Institut Curie, PSL Research University, Paris, France. ⁷Department of Surgical Oncology, Institut Curie, PSL Research University, Paris, France. ⁸Dermatology Department, Hôpital Saint André Centre Hospitalier Universitaire, Bordeaux, France. ⁹Medical Oncology Department, Centre Eugène Marquis, Rennes, France. ¹⁰Medical Oncology Department, Oscar Lambret Center, Lille, France. ¹¹Department of Medical and Surgical Oncology & Hematology, ICANS, Strasbourg, France. ¹²Department of Translational Research, Institut Curie, PSL Research University, Paris, France. ¹³UVSQ, Paris-Saclay University, Saint Cloud, France. e-mail: marc-henri.stern@curie.fr; shufang.renault@curie.fr

enhanced, HLA-A*02:01-restricted, T-cell receptor specific for a gp100-derived peptide fused to an anti-CD3 single-chain variable fragment that can recruit and activate polyclonal T-cells. Although tebentafusp showed an OS benefit in IMCgp100-202, the randomized phase 3 trial (NCT03070392)³, its efficacy in the real-world setting remains elusive. Importantly, tumor responses according to RECIST criteria⁴ were observed in only a fraction of patients (~10%) and discrepancies between radiographic response and OS were reported^{3,5}. Therefore, easily accessible, sensitive and specific methods allowing a better monitoring of individuals with metastatic UM (MUM) treated with tebentafusp in real-life are needed.

Circulating tumor DNA (ctDNA), a portion of total circulating cell-free DNA (ccfDNA), has become a pivotal biomarker for diagnosing, predicting outcomes, and monitoring treatment efficacy in various cancer types^{6,7}. UM provides an interesting model for testing ctDNA detection, due to the almost consistent presence of clonal, hotspot mutations, predominantly involving *GNAQ*, *GNA11*, *SF3B1* or *PLCB4* and *CYSLTR2* to a lesser extent⁴. Prior evidence from our group and others demonstrated the detectability of ctDNA in individuals affected with MUM using either droplet digital PCR (ddPCR) or targeted next-generation sequencing (NGS)^{8–12}. Both approaches have high sensitivity and specificity, each with its own advantages and limitations in detecting mutations. ddPCR requires to know the tumor mutational status before ctDNA detection to use the specific primers of the targeted mutations, but is cheaper, with faster turnaround time and independently of bioinformatics analyzes. In contrast, targeted NGS is agnostic and allows a larger panel of detected mutations, possibly with a global copy number profile. Therefore, the choice between these approaches will depend on the objectives of the study, the availability of the respective technologies, and the expected mutations in the tumor.

Exploratory analyzes from the phase 2 IMCgp100-102 and phase 3 IMCgp100-202 tebentafusp clinical trials^{3,5} suggest that detecting circulating tumor DNA (ctDNA) with a multiplex PCR-based targeted NGS panel in these trials, holds promise as an early predictive indicator of tebentafusp clinical efficacy. Significantly, the dynamics of ctDNA monitoring appeared particularly relevant in patients with progressive disease (PD) at first assessment as the patients with PD and paradoxical ctDNA decrease derived a clinical benefit from tebentafusp compared to those receiving the standard treatment¹³.

In this work, we report a prospective evaluation of ctDNA using ddPCR, an alternative cost-effective approach, in MUM patients treated with tebentafusp, showing the prognostic value of ctDNA at baseline, and the association between early ctDNA reduction and OS.

Results

Clinical characteristics of the patients

Sixty-nine individuals, diagnosed with MUM and eligible for tebentafusp treatment, were enrolled from January 2019 to December 2022 in this study. Median age was 59 years (range [51–66]) and 58% were women. Among the participants, 64% (44 patients) had not received any prior lines of therapy, and 86% (59 patients) presented solely with liver metastases at the initiation of tebentafusp therapy. Of 69 patients, 29 (42%) had their largest metastasis diameter superior to three centimeters (*i.e.* M1b/M1c according the TNM classification)¹⁴. Thirty-one patients out of 68 (46%) had elevated baseline serum lactate dehydrogenase (LDH). Genomic profiling revealed monosomy 3 in 83% of the patients with available data (57/69). Patient characteristics are detailed in Table 1 and Supplementary Table 1. ctDNA positivity was associated with number of previous lines of therapy, baseline serum LDH levels, diameter of the largest metastasis and best tumor response to tebentafusp based on imaging. Interestingly, all patients with partial response according to modified RECIST criteria had undetectable ctDNA at baseline (Table 1).

Patients' outcome

With a median follow-up of 20.0 months (interquartile range [IQR]: 15.2–23.2 months), disease progression was observed in 52 patients (75%) and deaths in 32 patients (46%). Metastatic UM was the cause of all deaths. The median PFS and OS achieved with tebentafusp were 2.8 months (95%CI [2.6–10.5]) and 21.8 months (95%CI [18.5–Not reached; NR]), respectively (Fig. 1A). The objective response rate (ORR) was 10% ($n = 7/68$), all being partial responses (PR), one patient was not evaluable because lesions were too small. Notably, 34% patients ($n = 23$) achieved stable disease (SD) as best overall response, while 56% ($n = 38$) experienced progressive disease (PD).

Identification of trackable somatic mutations

Of the 69 patients, archival tumor tissue from either the primary tumor or resected liver metastases was available for 67 individuals (97%). For the remaining two patients with no tumor tissue available for analysis, plasma ccfDNA at baseline served as the source for identifying somatic mutations. Ultimately, 97% of the cohort (67 out of 69 patients) harbored at least one trackable somatic mutation, in *GNAQ* ($n = 37$), *GNA11* ($n = 29$) or *SF3B1* ($n = 1$). Subsequently, these patients underwent assessment for ctDNA levels at baseline before tebentafusp, at 3 weeks (3w), 12 weeks (12w) and at progression, targeting the previously identified mutations.

Prognostic value of ctDNA detection at baseline, 3 weeks, 12 weeks

Among the 67 patients with trackable mutation, plasma samples were available for 65 at baseline and 64 were evaluable (one patient had less than 300 amplifiable genomes with no ctDNA detected; Fig. 1B). ctDNA was detectable in 39 out of 64 patients (61%) with a median of 31 copies/mL of plasma (IQR = 9–557 copies/mL of plasma; Fig. 2A). As tumor burden influences ctDNA levels¹⁵, ctDNA levels were positively correlated with serum LDH levels (Fig. 2B) and diameter of the largest metastasis (Fig. 2C). Notably, four patients with M1a disease (largest metastasis of less than three centimeters) paradoxically presented with high levels of ctDNA (>100 copies/mL of plasma). Three of these four patients presented with innumerable, small liver metastases, including one individual who also had countless bone metastases scattered throughout the spine (ctDNA: 9443 copies/mL of plasma), demonstrating that TNM does not perfectly reflect tumor burden. Conversely, the fourth patient (ctDNA: 112 copies/mL of plasma) exhibited only one visible liver metastasis, which was not extensively necrotic, indicating the potential presence of undetectable metastases elsewhere. In contrast, two patients with M1b disease were ctDNA negative at baseline. The remaining 23 ctDNA negative cases were M1a, as expected. All M1c cases were ctDNA positive. Interestingly, all patients with tumor response to tebentafusp had no ctDNA detected at baseline (7/25; 28% of ctDNA negative patients; Table 1).

By three weeks, 31 out of 64 patients (48%) tested positive for ctDNA (Fig. 2D). Of the 61 patients with paired plasma samples at baseline and 3w, 22 (36%) showed no ctDNA detection at either time point. Among the 36 patients with baseline ctDNA presence, 24 (67%) displayed reduced ctDNA levels at 3 weeks, with eight achieving complete ctDNA clearance. At the 1st tumor assessment (12w), 21 out of 56 patients (38%) had detectable ctDNA (median timing for ctDNA sampling = 12.0 weeks [IQR: 11.9–12.6]). Among the 54 paired samples (baseline and 12w), 22 patients (41%) showed no detectable ctDNA at both time points, including 19 who had also no detectable ctDNA at 3w (Fig. 2E). For patients initially exhibiting ctDNA, 22/31 (71%) experienced decreased ctDNA levels at 12 weeks, including 11 achieving complete ctDNA clearance. Seventeen patients had available plasma samples at disease progression, with 14 testing positive for ctDNA (Fig. 2E).

Patients with detectable ctDNA before treatment displayed significantly shorter PFS (median 2.5 months *versus* 10.8 months;

Table 1 | Clinical characteristics of the patients according to ctDNA positivity at baseline

Characteristics	Overall, n (%)	ctDNA unavailable, n (%)	ctDNA positive, n (%)	ctDNA negative, n (%)	<i>p</i> value ctDNA ^{pos} vs ctDNA ^{neg}
N patients	69 (100%)	5 (7%)	39 (57%)	25 (36%)	
Age, median (IQR)	59 (51, 66)	57 (51, 73)	61 (56, 66)	57 (47, 64)	0.2
Gender					0.5
Male	29 (42%)	4 (80%)	14 (36%)	11 (44%)	
Female	40 (58%)	1 (20%)	25 (64%)	14 (56%)	
Prior number of lines of therapy					0.05
0	44 (64%)	5 (100%)	20 (51%)	19 (76%)	
≥1	25 (36%)	0 (0%)	19 (49%)	6 (24%)	
Baseline serum LDH, N = 68					0.002
Normal	37 (54%)	4 (80%)	14 (37%)	19 (76%)	
Elevated	31 (46%)	1 (20%)	24 (63%)	6 (24%)	
Chromosome 3					0.2
Disomy 3	12 (17%)	2 (40%)	8 (21%)	2 (8%)	
Loss of heterozygosity	57 (83%)	3 (60%)	31 (79%)	23 (92%)	
Diameter of the largest metastasis according to TNM					0.000025
M1a	40 (58%)	4 (80%)	13 (33%)	23 (92%)	
M1b/c	29 (42%)	1 (20%)	26 (67%)	2 (8%)	
Sites of metastases at tebentafusp initiation					0.5
Liver	59 (86%)	5 (100%)	32 (82%)	22 (88%)	
Liver + Other	10 (14%)	0 (0%)	7 (18%)	3 (12%)	
Best response, N = 68					0.002
PD	38 (56%)	2 (40%)	27 (71%)	9 (36%)	
PR	7 (10%)	0 (0%)	0 (0%)	7 (28%)	
SD	23 (34%)	3 (60%)	11 (29%)	9 (36%)	
SF3B1, N = 62					0.4
No	51 (82%)	3 (100%)	28 (78%)	20 (87%)	
Yes	11 (18%)	0 (0%)	8 (22%)	3 (13%)	
BAP1, N = 61					0.2
No	15 (25%)	2 (50%)	10 (29%)	3 (13%)	
Yes	46 (75%)	2 (50%)	24 (71%)	20 (87%)	
EIF1AX, N = 59					
No	59 (100%)	3 (100%)	33 (100%)	23 (100%)	

IQR: interquartile range; N: number of patients available; PD: progressive disease; PR: partial response, SD: stable disease. ctDNA^{pos}: ctDNA positive; ctDNA^{neg}: ctDNA negative. Categorical variables were compared using Pearson's Chi-squared test or Fisher's exact test. For continuous variables, Wilcoxon rank sum tests were employed. Two-sided statistical tests were used. *P* values ≤ 0.05 are indicated as bold formatting in the table.

HR = 2.8, 95% CI [1.5-5.2], *p* = 0.001) and OS (median 12.9 months *versus* 40.5 months; HR = 10.1, 95% CI [3.0-33.8]; *p* < 0.001; Fig. 3A). The observed difference in OS between the two groups was not attributed to treatments administered after the interruption of tebentafusp, as the distribution of post-tebentafusp therapies, including PD1 inhibitors, was balanced across groups regardless of ctDNA detection at baseline (Supplementary Table 2). Furthermore, ctDNA detection at 3w and 12w were correlated also with poorer prognoses in both PFS (*p* < 0.001 for both 3w and 12w) and OS (*p* < 0.001 both; Supplementary Fig. 1). Finally, baseline LDH and tumor burden according to TNM were also associated with prognosis (Fig. 3B and C).

ctDNA dynamics as a pharmacodynamic marker

Among the 19 patients with no ctDNA detection at baseline, 3w and 12w, 11 (58%) had SD and eight (42%) had PD at the first tumor assessment. Fourteen of the 22 patients with ctDNA decrease between baseline and 12w, had PD at first assessment (64%; Supplementary Fig. 2A). More precisely, among the 11 patients achieving complete ctDNA clearance at 12w, five (45%) had SD and six had PD (55%). A

smaller proportion of patients had already cleared their ctDNA at three weeks (three (*n* = 3/8, 37.5%) with SD, five (*n* = 5/8, 62.5%) with PD; Supplementary Fig. 2B). Using less stringent thresholds, 90% and 50% of ctDNA decrease, for defining ctDNA decrease at 12w revealed a higher number of patients classified as PD while exhibiting a reduction in ctDNA (*n* = 7/13, 54% for 90% decrease and *n* = 9/16, 56% for 50% decrease, respectively). Notably, among the 22 patients with PD and ctDNA variation in paired samples, nine displayed a minimum of 50% reduction in ctDNA levels, with six achieving complete ctDNA clearance.

Regarding survival outcomes, ctDNA-positive patients at baseline who experienced complete clearance at 12 weeks (*n* = 11) had a significantly longer median OS (12.7 months *versus* 34.6 months; HR = 7.1, 95% CI [1.6-31.4], *p* = 0.003) and PFS (2.6 months *versus* 17.1 months; HR = 2.9, 95% CI [1.1-8.0], *p* = 0.03) compared to those without clearance (*n* = 21; Fig. 4A and Supplementary Fig. 3A). Similar trends were observed with different thresholds. Patients achieving a 90% ctDNA decrease at 12w (*n* = 13) *versus* those who did not (*n* = 19) had a longer median OS (12.9 months *versus* 21.2 months; HR = 3.4, 95% CI [1.1-10.4],

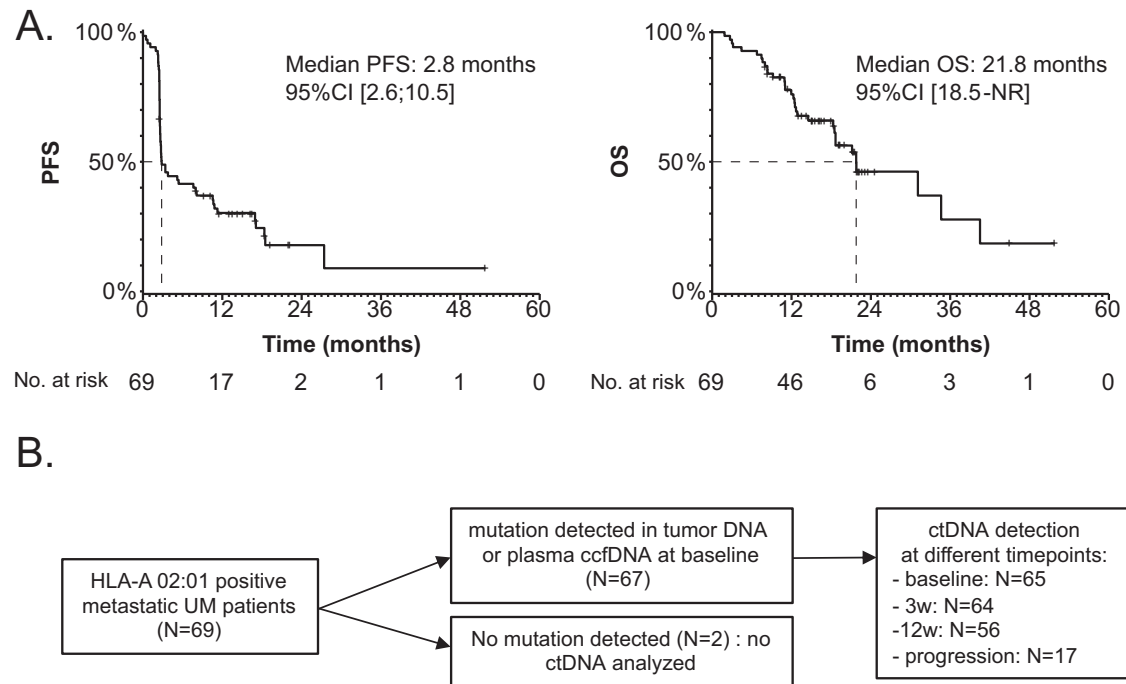


Fig. 1 | Progression-free survival (PFS) and overall survival (OS) in the whole cohort (A) and workflow (B). Patients in the PFS curve are censored at the date of last news if not in progression, while patients in the OS curve are censored at the

date of last news if alive. NR: not reached; UM: uveal melanoma; 3w: 3 weeks; 12w: 12 weeks. Source data are provided as a Source Data file.

$p=0.02$) and longer median PFS (2.6 months *versus* 10.6 months; HR=2.6, 95%CI [1.1-6.5], $p=0.03$). When a 50% threshold at 12w was applied, a numerically longer OS (median 12.9 months for the 16 patients with 50% decrease *versus* 21.2 months for the 16 others, $p=0.07$) and PFS (2.7 months *versus* 6.7 months; $p=0.09$) were observed though not statistically significant. No significant result was observed between baseline and 3w (Fig. 4B and Supplementary Fig. 3B). Importantly, among patients with PD, clearance of ctDNA at 12w ($n=6$) demonstrated a longer OS compared to patients without ctDNA clearance ($n=16$; median OS of 12.5 *versus* 21.2 months; HR = 6.3, 95%CI [1.3-27.8], $p=0.009$), which was comparable to those who tested negative for ctDNA at baseline (Fig. 4C). It is worth noting that only a limited number of patients was available for this analysis.

Univariate and multivariate analyzes

Univariate and multivariate proportional hazards models were performed in the cases with matched samples at baseline and 12w ($n=54$) to assess the prognostic significance of clinicopathological factors, in combination with ctDNA detection at different time points and ctDNA variation. As shown in Supplementary Table 3, ctDNA detection at baseline, 3w or 12w, and ctDNA clearance between baseline and 12w were significantly associated with PFS and OS in univariate analyzes, while prior number of lines of therapy, elevated baseline serum LDH and diameter of the largest metastasis according to TNM were only associated with OS.

In multivariate analyzes, two models were constructed for PFS and OS analyzes. In Model 1 (which integrates a “detection of ctDNA at baseline” variable), baseline ctDNA positivity emerged as an independent prognostic factor for OS and PFS (for OS: HR = 9.3, 95%CI [1.9-45.2], $p=0.006$ and for PFS: HR = 2.5, 95%CI [1.1-5.9], $p=0.04$, respectively) while elevated LDH level was only associated with OS (HR = 4.4, 95%CI [1.5-13.4], $p=0.008$), as detailed in Table 2. In Model 2, patients with ctDNA positivity at baseline who either cleared ctDNA by 12 weeks or did not were compared against patients who were ctDNA-negative both at baseline and at 12 weeks (reference group). This comparison aimed to evaluate if achieving ctDNA clearance by

12 weeks translated to similar PFS and OS outcomes as being ctDNA-negative from the start, and how these outcomes compared to patients with persistent ctDNA positivity. No statistically significant difference in PFS or OS was found between patients with ctDNA clearance at 12 weeks and the reference group (HR = 1.7, 95% CI [0.6-4.8], $p=0.3$ and HR = 6.8, 95% CI [0.7-69.2], $p=0.1$, respectively). In contrast, patients with persistent ctDNA positivity at 12 weeks had significantly worse PFS and OS compared to the reference group (HR = 5.8, 95% CI [2.1-16.5], $p=0.0009$ and HR = 49.6, 95% CI [4.5-544.5], $p=0.001$, respectively).

Additionally, changing the reference group in model 2 for patients who were ctDNA-positive at baseline and remained positive at 12 weeks, those who did not achieve ctDNA clearance at 12 weeks had significantly worse PFS and OS than those who achieved ctDNA clearance (HR = 3.5, 95%CI [1.3-9.1], $p=0.01$ and HR = 7.3, 95%CI [1.4-37.1], $p=0.02$).

Discussion

Tebentafusp was the first systemic treatment to demonstrate a meaningful OS benefit in metastatic UM patients. With an ORR of 10% and a median OS of 22 months, our study’s outcomes closely mirror those reported in the IMCgp100-202 phase 3 trial³, which demonstrated an ORR of 11% and an OS of 22 months. These consistent findings across more diverse patient populations and different treatment lines underscore the drug’s relevance and effectiveness in clinical practice.

Our main goal was the evaluation of ctDNA detection using ddPCR in MUM patients treated with tebentafusp. In this series, 61% of MUM patients exhibited detectable ctDNA in plasma prior to tebentafusp treatment initiation. Notably, our findings revealed the same rate of detectable ctDNA compared to the IMCgp100-202 trial, in which ctDNA was assessed with a dedicated multiplex PCR-based NGS panel. However, an essential distinction lies in the patient selection criteria between our series and the clinical trial setting. In our study, we treated patients with different tumor burdens, often including those with the lowest tumor burdens in our daily practice, in contrast to the trial’s

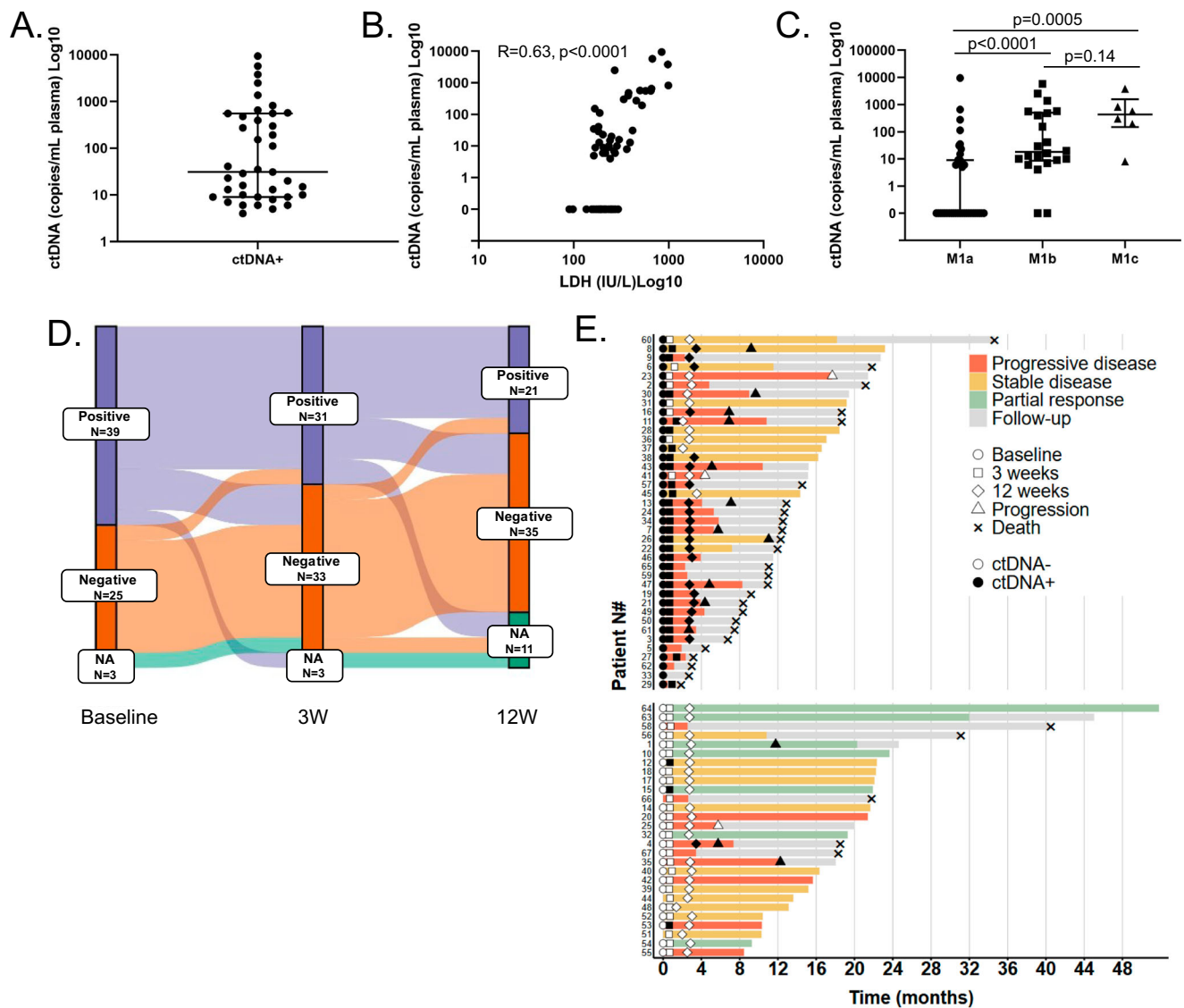


Fig. 2 | ctDNA detection before and on treatment. **A** levels of ctDNA detection at baseline in patients with ctDNA detected ($n = 39$, median = 31.0, IQR [9.0-557.0]). Error bars are presented as median \pm IQR. **B**, **C** correlation between baseline ctDNA levels with serum LDH level (Pearson coefficient; **B**); $n = 63$, exact p -value: 3.10^{-8}) and with diameter of the largest metastasis according to TNM (Wilcoxon test; **C**); M1a: $n = 36$; M1b: $n = 22$ and M1c: $n = 6$). Error bars are presented as median \pm IQR. M1a: median = 0.1, IQR [0.1-9.0]; M1b: median = 18.0, IQR [8.5-499.3]; M1c: median = 431.0, IQR [146.8-1570]. Two-sided statistical tests were used. Exact p -value for comparison between M1a and M1b is $9.6.10^{-5}$. **D** Sankey plot showing the dynamic changes of ctDNA detection in patients under tebentafusp.

E swimmer plot showing the dynamic changes of ctDNA levels in each patient. Top panel E presents the patients with ctDNA detected at baseline while bottom panel presents patients without ctDNA detected at baseline or patients with no available ctDNA analysis at baseline. Symbols in black and white represent the samples with positive and negative ctDNA detection. Red, yellow and green bars represent the duration of treatment (with colors representing the best response in each patient) while gray bars represent the follow-up after tebentafusp discontinuation. ND: not detected; LDH: lactate dehydrogenase; MAF: mutant allele frequency; NA: not available; TNM: tumor node metastasis classification. Source data are provided as a Source Data file.

inclusion criteria requiring RECIST-measurable lesions. However, the tumor burden in our series resembled that of the IMCgp100-202 trial, with 42% of patients showing a largest metastatic lesion exceeding 3 cm (compared to 42% in the trial) and 46% exhibiting LDH levels surpassing the normal range (compared to 30% of patients evaluable for ctDNA in IMCgp100-202). These parallels imply that ddPCR demonstrates comparable sensitivity to the multiplex PCR-based NGS panel utilized in the trial specifically designed to detect seven hotspot mutations at very low mutant allelic frequency (MAF). It is noteworthy that the sensitivity of NGS panels is inherently tied to the size of the captured or amplified regions, meaning that larger panels, including whole-exome, may offer reduced sensitivity in detecting ctDNA.

Similar to high LDH levels, detection of ctDNA at baseline was associated with a poor median OS, emphasizing its potential as a

prognostic marker. ctDNA levels were positively associated with tumor burden as appraised by TNM in most cases. However, discrepancies were observed in some cases (*i.e.* high levels with limited tumor burden or low levels with bulky lesions) suggesting that ctDNA assay may capture biological factors influencing it beyond tumor burden, such as proliferation and necrosis. An important observation in this work is that not only was the detection of ctDNA prognostic, but its presence also appeared to be predictive of the response to tebentafusp as all responders tested negative for ctDNA negative at baseline. More precisely, 28% of patients with no ctDNA detection at baseline presented a tumor response. Moreover, our study corroborates existing evidence linking ctDNA reduction during tebentafusp treatment with improved clinical outcomes. ctDNA reduction on other immune therapies such as checkpoint blockade has already been associated with better clinical

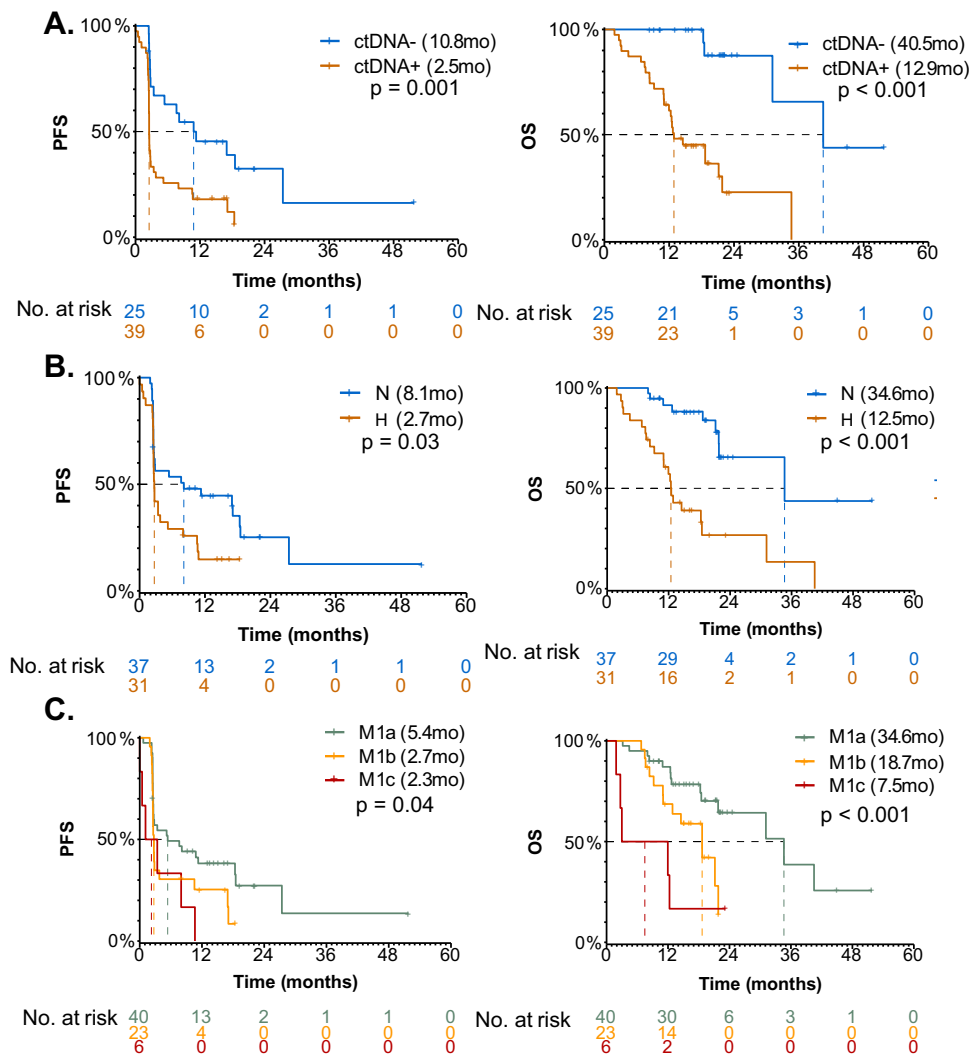


Fig. 3 | Prognostic values of ctDNA, LDH and TNM classification. Prognostic values of markers on PFS (left panels) and OS (right panels) at baseline.

A Prognostic value of ctDNA detection. Exact p -value for OS: 7.10^{-6} . **B** Prognostic value of LDH. Exact p -value for OS: 10^{-5} . **C** Prognostic value of TNM. Exact p -value

for OS: 7.10^{-4} . N: normal range; H: higher than normal range; PFS: Progression Free Survival; OS: Overall Survival. Kaplan–Meier plots were used for survival analysis, with significance assessed using the two-sided log-rank test. Source data are provided as a Source Data file.

outcomes in multiple studies^{16–18}. Similarly, ctDNA clearance at nine weeks of tebentafusp in IMCgp100-202 using multiplex PCR-based NGS was associated with better OS (median OS from week nine, 29.6 months *versus* 10.2 months)³. In our study, a substantial reduction by 90% in ctDNA levels at 12 weeks also showed a significant association with increased OS. Lower threshold (*i.e.* 50%) or earlier ctDNA clearance (*i.e.* 3 weeks) were associated with lower predictive values in our series as well as in the phase 3 trial, highlighting the importance of standardizing monitoring not only time points but also thresholds for accurate comparisons. Further studies with more frequent longitudinal blood sampling during the first cycles might be of interest to clarify the best time points of ctDNA sampling. Notably, while traditional radiographic response criteria, such as RECIST, may underestimate the benefit from tebentafusp^{3,5}, our observations support the use of ctDNA clearance at 12 weeks as a predictive biomarker, particularly in patients with progressive disease. Similarly, clearance of ctDNA at 12 weeks demonstrated a longer OS in patients with PD, comparable to that of patients tested negative for ctDNA at baseline. However, this needs to be confirmed in independent series.

In our study, ddPCR compared favorably with targeted NGS in detecting ctDNA. Indeed, with the development of multiplex PCR-based targeted NGS, detecting ctDNA in plasma at very low frequency is now reachable, as shown in the IMCgp100 trials. Furthermore, this method has the advantage of being mutation-agnostic, which can be crucial in tumor types with heterogeneous drivers. However, UM is characterized by specific and frequent hotspot mutations, notably *GNAQ* and *GNAI1* mutated in 85% of UM cases. Therefore, UM is a most favorable tumor type for ctDNA detection via ddPCR. Our study highlights the feasibility of the following pipeline identifying first somatic mutations through targeted tumor sequencing, followed then by highly sensitive ctDNA detection using ddPCR. Compared to multiplex PCR-based NGS, this procedure is easily implementable, cost-effective, with a short turnaround time, making this method suitable for clinical applications in most hospitals. Importantly, further developments of multiplex ddPCR assays encompassing the main UM hotspot mutations should allow a mutation-agnostic approach in the next future. We thus believe that ddPCR should be considered as the

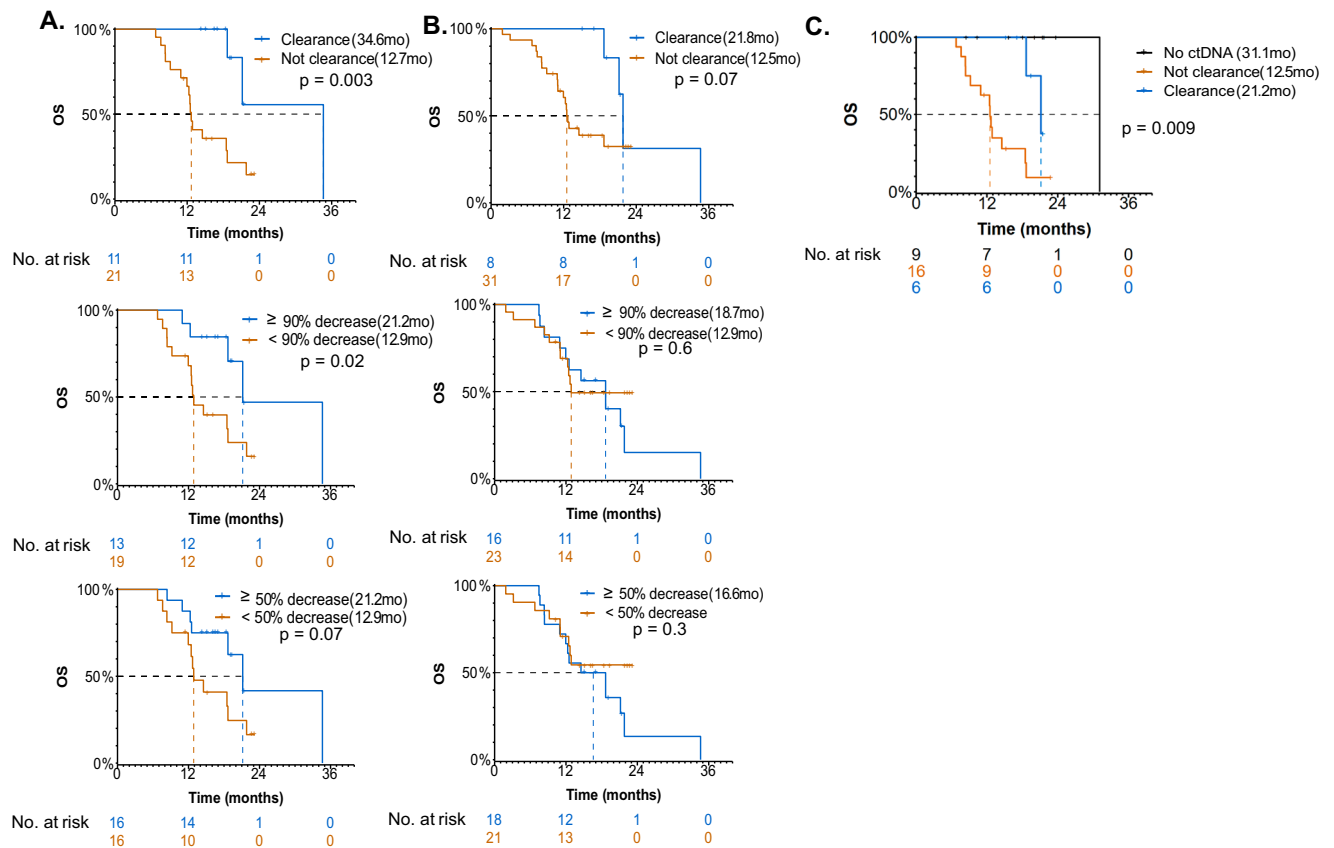


Fig. 4 | Predictive value of ctDNA variations on tebentafusp. According to variation at 12 weeks (A) 3 weeks (B) and 12 weeks in patients with progressive disease at first assessment (C). OS: overall survival. Clearance of ctDNA is defined as the absence of detectable ctDNA at 3 weeks or 12 weeks after treatment, following an

initial detection of ctDNA at baseline. Kaplan–Meier plots were used for survival analysis, with significance assessed using the two-sided log-rank test. Source data are provided as a Source Data file.

Table 2 | Multivariate analysis for PFS and OS

Variables	Model 1			Model 2		
	HR	95% CI	p value	HR	95% CI	p value
Progression-free survival						
At least one previous line of treatment (versus 0 line)	0.8	0.4–1.9	0.6	0.8	0.3–1.7	0.5
Elevated baseline LDH (versus normal)	0.9	0.4–1.9	0.8	0.7	0.3–1.4	0.3
Diameter of the largest metastasis according to TNM (M1b/c versus M1a)	1.0	0.4–2.5	1.0	0.8	0.3–1.9	0.6
ctDNA detection at baseline (versus negative)	2.5	1.1–5.9	0.04	/	/	/
ctDNA clearance at 12w (versus negative at baseline and 12w)						
Yes	/	/	/	1.7	0.6–4.8	0.3
No	/	/	/	5.8	2.1–16.5	0.0009
Overall survival						
At least one previous line of treatment (versus 0 line)	0.6	0.4–1.9	0.4	0.6	0.2–1.7	0.3
Elevated baseline LDH (versus normal)	4.4	1.5–13.4	0.008	2.1	0.7–6.2	0.2
Diameter of the largest metastasis according to TNM (M1b/c versus M1a)	0.8	0.2–2.5	0.7	0.9	0.3–2.6	0.8
ctDNA detection at baseline (versus negative)	9.3	1.9–45.2	0.006	/	/	/
ctDNA clearance at 12w (versus negative at baseline and 12w)						
Yes	/	/	/	6.8	0.7–69.2	0.1
No	/	/	/	49.6	4.5–544.5	0.001

Model 1 integrates ctDNA detection at baseline while model 2 does not and includes ctDNA variation at 12 weeks. 12w: 12 weeks; CI: Confidence Interval; HR: Hazard Ratio. Cox proportional hazards modeling, encompassing univariate and multivariate analyzes, evaluated the prognostic significance of different predictors. Two-sided statistical tests were used. P values ≤ 0.05 are indicated as bold formatting in the table. No formal adjustment for multiplicity was performed.

method of choice when implementing routine ctDNA for MUM patients.

Intriguingly, although the limited number of patients and high proportion of monosomy 3 in our cohort prevent any definitive conclusion, this genomic alteration was not associated with prognosis in this cohort of metastatic patients. While monosomy 3 in primary tumors is consistently associated with a shorter time to first metastasis and subsequent shorter OS¹, its impact on survival in the metastatic setting is less clear. Moreover, given that monosomy 3 UM has been linked to higher immune infiltrate¹, it raises the possibility that specific immunological features associated with monosomy 3 might sensitize these tumors to tebentafusp. In fact, six out of the seven patients with partial response had monosomy 3, while the genomic profile was unavailable for the last patient. Again, the fact that 83% of the whole cohort was monosomy 3 prevents any conclusion. This underscores the importance of further investigations into the interplay between biological markers and treatment response in this population.

In conclusion, our data reinforces the role of tebentafusp in patients with MUM and advocates for the use of ddPCR-based ctDNA monitoring as a practical, cost-effective approach directly applicable in routine. These findings offer a potential avenue for treatment de-escalation (limited course of tebentafusp instead of pursuing it until progression) or intensification (combination studies) based on ctDNA dynamics, paving the way for personalized therapeutic strategies in the management of UM.

Methods

Patients

The study was performed in accordance with the ethical principles of the Declaration of Helsinki, the International Conference on Harmonization/Good Clinical Practice guidelines, and the Public Health Code in France. All patients enrolled in ALCINA study (NCT02866149) provided written informed consent. The ALCINA study received a favorable opinion from the French national ethics committee “Comité de Protection des Personnes Ile-De-France VI”. All patients included were HLA-A*02:01-positive and were treated with tebentafusp. The treatment regimen comprised intravenous administration of tebentafusp at an initial dose of 20 µg in week 1, followed by 30 µg in week 2, and a subsequent weekly dosage of 68 µg. Tumor response was assessed by mandatory liver MRI at 12-week intervals interpreted according to modified RECIST v1.1 criteria (target lesions ≥5 millimeters) and RECIST v1.1 criteria⁴ on thoraco-abdomino-pelvic CT scan, categorizing responses as complete response (CR), partial response (PR), stable disease (SD), or progressive disease (PD) by UM expert radiologists. Tebentafusp could be pursued beyond radiographic progression in asymptomatic patients with non-threatening PD at first assessment (12w) according to irRECIST¹⁹ with an early new assessment four to eight weeks after, as done in the IMCgp100-202 study. LDH measurement was conducted as part of routine clinical practice in external laboratories, and as such, the specific method employed varied between facilities. Chromosome 3 assessment was also conducted as part of routine clinical practice. Its status was retrieved from testing on metastases whenever possible, or by default in primary tumors when available.

Blood sampling and plasma sample preparation, storage, DNA extraction and quantification

Blood samples were obtained longitudinally at specific intervals: prior to treatment initiation, cycle 2 (after 3 weeks of treatment; 3w), at the first tumor assessment (cycle 5, after 12 weeks of treatment; 12w), and at the time of disease progression. EDTA tubes were used for blood collection. Following blood collection, EDTA tubes were promptly transported at room temperature to the local laboratory for plasma isolation. Within 2 hours, plasma was isolated through a two-step centrifugation process: 820 g for 10 minutes, followed by 16,000 g for

10 minutes at 4 °C and then stored at –80 °C until use. DNA extraction from plasma samples was performed using the QIAmp Circulating Nucleic Acid Kit (Qiagen, Hilden, Germany) following the manufacturer’s instructions. The quantification of extracted DNA was conducted using the dsDNA HS Assay on a Qubit 2.0 fluorometer (Invitrogen, Carlsbad, CA, USA). Extracted DNA samples were stored at –20 °C until further analysis.

Mutation detection with the use of ddPCR assays

Sequencing was conducted using an in-house NGS panel targeting *GNAQ*, *GNAI1* and *SF3B1* on archived tumor DNA (primary tumor or metastases) but for two cases with no tumor DNA available, for whom plasma ccfDNA at baseline was used. Subsequently, the identified mutations in *GNAQ*, *GNAI1*, or *SF3B1* were employed for ctDNA monitoring in plasma using droplet digital PCR (ddPCR). *BAP1* mutations were not selected as they are distributed throughout the gene without a specific hotspot, making them suboptimal for ctDNA follow-up using ddPCR. First, to validate our assays, DNA from cell lines including OMM2.3 (*GNAQ* p.Q209P c.626 A > C), MP46 (*GNAQ* p.Q209L c.626 A > T), OMM1 (*GNAI1* p.Q209L c.626 A > T)^{20–22}, and tumor tissues carrying mutations such as *GNAQ* p.Q209R c.626 A > G, *GNAQ* p.R183Q c.548 G > A, *GNAI1* p.R183C c.547 C > T, *SF3B1* p.R625C c.1873C > T, *GNAQ* p.Q209L c.625_626delCAinsTT, and *GNAQ* p.Q209H c.627 A > C were used as positive controls. Genomic DNA from healthy donors procured from Promega (Madison, WI, USA) served as negative controls. Assays for detecting *GNAQ* p.Q209L c.626 A > T, *GNAI1* p.Q209L c.626 A > T, *GNAQ* p.Q209R c.626 A > G, *GNAQ* p.R183Q c.548 G > A, and *GNAI1* p.R183C c.547 C > T were procured from Bio-Rad laboratories (Hercules, CA, USA). For the detection of *GNAQ* p.Q209P c.626 A > C, *GNAQ* p.Q209L c.625_626delCAinsTT, *GNAQ* p.Q209H c.627 A > C and *SF3B1* p.R625C c.1873 C > T mutations, specific primers and probes are detailed in Supplementary Table 4 and Supplementary Table 5.

The ddPCR assays were performed using the BioRad QX100 system following standardized protocols. The reaction conditions involved the use of specific primer and probe concentrations, with one probe targeting the wild-type sequence and the other targeting the mutant sequence, each labeled with different fluorophores. Amplification conditions included an initial cycle at 95 °C for 10 minutes, followed by 40 cycles at 94 °C for 30 seconds and hybridization at mutation-specific temperatures for 60 seconds, concluding with a cycle at 98 °C for 10 minutes. Cluster thresholding and quantification were executed using QuantaSoft v.1.7.4 software. Droplets were manually classified as wild-type (WT) or mutant (MUT) based on their fluorescence amplitude: WT (VIC+ or HEX+) and MUT (FAM+). The mutant allelic frequencies (MAFs) were calculated as the copy numbers of MUT divided by the sum of the copy numbers of WT and MUT, determining the total copy number of ccfDNA in each patient. For patients lacking somatic mutation status, custom ddPCR assays were employed to detect somatic mutations in either tumor DNA or plasma ccfDNA at baseline. All experiments adhered to the minimum requirements for digital PCR data^{23,24}.

ddPCR data analysis

The false-positive rate for each assay was estimated using ≥ 19 replicates of wild-type (WT) DNA, as previously described^{25,26}. The limit of blank (LOB), defined as the upper 95% confidence limit of mean false-positive measurements, was determined as follows: 0.012% for *GNAQ* p.Q209P c.626 A > C, 0.006% for *GNAQ* p.Q209L c.626 A > T, 0.005% for *GNAQ* p.Q209R c.626 A > G, 0.008% for *GNAQ* p.R183Q c.548 G > A, 0.018% for *GNAI1* p.R183C c.547 C > T, 0.00% for *GNAI1* p.Q209L c.626 A > T, 0.02% for *GNAQ* p.Q209L c.625_626delCAinsTT, *GNAQ* p.Q209H c.627 A > C, and 0.04% for *SF3B1* p.R625C c.1873C > T. Analytical sensitivity was determined using serial dilutions of mutation-carrying DNA in WT DNA (total input DNA: 15 ng), with MAFs ranging

from 0.50 to 0.01%. The limit of detection (LOD) was defined as the lowest mutant ratio reliably distinguishable from the LOB value. Samples were considered positive when the MAF exceeded the LOD, with specific positive droplet counts required per mutation type: more than 3 positive droplets for *SF3B1* p.R625C c.1873C>T, 2 positive droplets for *GNAQ* p.Q209L c.625_626delCAinsTT, p.Q209H c.627 A>C, and *GNAI1* p.R183C c.547C>T, or 1 positive droplet for *GNAQ* p.Q209P c.626 A>C, p.R183Q c.548 G>A, p.Q209L c.626 A>T, p.Q209R c.626 A>G, and *GNAI1* p.Q209L c.626 A>T per analysis. Samples with fewer than 300 amplifiable genomes and no ctDNA detected by ddPCR were excluded from further ctDNA analysis.

Statistical analyzes

Categorical variables were compared using Pearson's Chi-squared test or Fisher's exact test. For continuous variables, Mann-Whitney test and Wilcoxon rank sum tests were employed. Pearson coefficient was used for assessing correlations. Kaplan–Meier plots were used for survival analysis, with significance assessed using the logrank test. PFS was defined as the time from tebentafusp initiation to disease progression or death. Patients without disease progression were censored at their last follow-up visit. OS was defined as the time from tebentafusp commencement to death from any cause. Cox proportional hazards modeling, encompassing univariate and multivariate analyzes, evaluated the prognostic significance of different predictors. Model 1 assessed variables with a p -value < 0.1 in univariate analysis, including ctDNA detection at baseline and other relevant pathological characteristics. Model 2 replaced ctDNA detection at baseline with ctDNA clearance at 12 weeks as an independent variable. Statistical analyzes were conducted using GraphPad Prism (version 8.0) or R software (version 4.1.1), two-sided p -values \leq 0.05 indicating statistical significance. No formal adjustment for multiplicity was performed.

Reporting summary

Further information on research design is available in the Nature Portfolio Reporting Summary linked to this article.

Data availability

All data used to generate the figures and tables in this study are available in the supplementary data files. Source data are provided with this paper.

Code availability

No custom codes or mathematical algorithms were used for the analysis and figure generation. All analyzes were performed on the R software using the following packages: survival, survminer, ggplot2, ggsankey, prodlim.

References

- Jager, M. J. et al. Uveal melanoma. *Nat. Rev. Dis. Prim.* **6**, 24 (2020).
- Khoja, L. et al. Meta-analysis in metastatic uveal melanoma to determine progression free and overall survival benchmarks: an international rare cancers initiative (IRCI) ocular melanoma study. *Ann. Oncol.* **30**, 1370–1380 (2019).
- Hassel, J. C. et al. Three-year overall survival with tebentafusp in metastatic uveal melanoma. *N. Engl. J. Med.* **389**, 2256–2266 (2023).
- Eisenhauer, E. A. et al. New response evaluation criteria in solid tumours: revised RECIST guideline (version 1.1). *Eur. J. Cancer* **45**, 228–247 (2009).
- Carvajal, R. D. et al. Clinical and molecular response to tebentafusp in previously treated patients with metastatic uveal melanoma: a phase 2 trial. *Nat. Med.* **28**, 2364–2373 (2022).
- Gerratana, L. et al. Emerging role of genomics and cell-free DNA in breast cancer. *Curr. Treat. Options Oncol.* **20**, 68 (2019).

- Cabel, L. et al. Clinical potential of circulating tumour DNA in patients receiving anticancer immunotherapy. *Nat. Rev. Clin. Oncol.* **15**, 639–650 (2018).
- Madic, J. et al. Pyrophosphorolysis-activated polymerization detects circulating tumor DNA in metastatic uveal melanoma. *Clin. Cancer Res.* **18**, 3934–3941 (2012).
- Bidard, F. C. et al. Detection rate and prognostic value of circulating tumor cells and circulating tumor DNA in metastatic uveal melanoma. *Int. J. Cancer* **134**, 1207–1213 (2014).
- Park, J. J., et al. Circulating tumor DNA reflects uveal melanoma responses to protein kinase C inhibition. *Cancers (Basel)* **13**, 1740 (2021).
- Shoushtari, A. N. et al. Early reduction in ctDNA, regardless of best RECIST response, is associated with overall survival (OS) on tebentafusp in previously treated metastatic uveal melanoma (mUM) patients. *Ann. Oncol.* **32**, S1210 (2021).
- Mariani, P. et al. Circulating Tumor DNA as a prognostic factor in patients with resectable hepatic metastases of uveal melanoma. *Ann. Surg.* **278**, e827–e834 (2023).
- Nathan, P. et al. Overall survival benefit with tebentafusp in metastatic uveal melanoma. *N. Engl. J. Med.* **385**, 1196–1206 (2021).
- Cancer, A. J. C. o. In: *AJCC Cancer Staging Manual* (ed[^](eds). 8th edn. Springer (2017).
- Postel, M., Roosen, A., Laurent-Puig, P., Taly, V. & Wang-Renault, S. F. Droplet-based digital PCR and next generation sequencing for monitoring circulating tumor DNA: a cancer diagnostic perspective. *Expert Rev. Mol. Diagn.* **18**, 7–17 (2018).
- Zhang, Q. et al. Prognostic and predictive impact of circulating tumor DNA in patients with advanced cancers treated with immune checkpoint blockade. *Cancer Discov.* **10**, 1842–1853 (2020).
- Raja, R. et al. Early reduction in ctDNA predicts survival in patients with lung and bladder cancer treated with durvalumab. *Clin. Cancer Res.* **24**, 6212–6222 (2018).
- Goldberg, S. B. et al. Early assessment of lung cancer immunotherapy response via circulating tumor DNA. *Clin. Cancer Res.* **24**, 1872–1880 (2018).
- Seymour, L. et al. iRECIST: guidelines for response criteria for use in trials testing immunotherapeutics. *Lancet Oncol.* **18**, e143–e152 (2017).
- Amirouchene-Angelozzi, N. et al. Establishment of novel cell lines recapitulating the genetic landscape of uveal melanoma and pre-clinical validation of mTOR as a therapeutic target. *Mol. Oncol.* **8**, 1508–1520 (2014).
- Chen, P. W. et al. Expression of MAGE genes in ocular melanoma during progression from primary to metastatic disease. *Clin. Exp. Metastasis* **15**, 509–518 (1997).
- Luyten, G. P. et al. Establishment and characterization of primary and metastatic uveal melanoma cell Lines. *Int. J. Cancer* **66**, 380–387 (1996).
- Huggett, J. F. et al. The digital MIQE guidelines: minimum information for publication of quantitative digital PCR experiments. *Clin. Chem.* **59**, 892–902 (2013).
- d, M. G., Huggett, J. F. The digital MIQE guidelines update: minimum information for publication of quantitative digital PCR experiments for 2020. *Clin. Chem.* **66**, 1012–1029 (2020).
- Jeannot, E. et al. A single droplet digital PCR for ESR1 activating mutations detection in plasma. *Oncogene* **39**, 2987–2995 (2020).
- Zonta, E., et al. Multiplex detection of rare mutations by picoliter droplet based digital PCR: sensitivity and specificity considerations. *PLoS One* **11**, e0159094 (2016).

Acknowledgements

This work was supported by SIRIC 2 Curie (grant INCa-DGOS-Inserm_12554). MR was supported by an Interface INSERM grant.

JLS is supported by the Swiss National Science Fund (P500PM_214231). The authors would like to thank Agathe Garcia for her invaluable assistance with patient data and the DRUM team and especially Olivier Ganier for fruitful scientific discussions. Additionally, they thank Leanne de Koning for her indispensable support throughout this research endeavor and more globally in UM research at Institut Curie. The authors also express their sincere thanks to the patients and their families whose participation and cooperation made this study possible and INCa for supporting the French MELACHONAT network.

Author contributions

M.R., M.H.S., S.R. designed the study; M.R., S.R. wrote the manuscript; A.R., J.L.S., A.H., M.R. and S.R. analyzed the data; T.R., V.S., L.M.G., G.P., V.S., A.V.S., N.C., P.M., C.D., M.P., T.R., J.E.K., S.P.N. and M.R. collected the clinical data; S.R.R. obtained the financial support for this study; F.C.B., S.P.N., M.H.S., M.R. and S.R. reviewed the manuscript.

Competing interests

M.R. reports personal fees for serving as an advisor from Merck Sharp & Dohme, AstraZeneca, GlaxoSmithKline, Immunocore; travel support from AstraZeneca; funds to his institution to support research from Merck Sharp & Dohme, Janssen-Cilag, Daiichi-Sankyo. F-C.B. received advisory board fees from Pfizer, AstraZeneca, Daiichi-Sankyo, Lilly, Novartis, Menarini, Caris Life Science, GE Healthcare, Exact Sciences, Gilead, Roche, SAGA Diagnostics; research support from AstraZeneca, Novartis, Pfizer, Prolynx, Merck KGaA, GE Healthcare, SAGA Diagnostics, Personalis; travel support from AstraZeneca, Novartis, Pfizer, Daiichi-Sankyo. A.V-S. received research grant from AstraZeneca, Daiichi-Sankyo, Ibex, Owkin, Prima; travel support from AstraZeneca, Roche; conference fees from Daiichi-Sankyo, Exactsciences, Amgen; honoraria for conferences or lectures from AstraZeneca, Roche, MSD, Exactsciences; advisory board or consultant fees from Ibex, Prima. M.P. received advisory board fees and travel support from AstraZeneca. J-E.K. reports personal fees for serving as an advisor from GlaxoSmithKline, Clovis Oncology, Tesaro, AstraZeneca, and Dragonfly Therapeutics; funds to his institution to support research from Merck Sharp & Dohme; travel support from Roche, PharmaMar, Tesaro. S.P-N reports personal fees for serving as an advisor from Immunocore and Pierre Fabre and travel support from Immunocore, Novartis. M-H.S. and S.R. received

research support from Immunocore. The remaining authors declare no competing interests.

Additional information

Supplementary information The online version contains supplementary material available at <https://doi.org/10.1038/s41467-024-53145-0>.

Correspondence and requests for materials should be addressed to Marc-Henri Stern or Shufang Renault.

Peer review information *Nature Communications* thanks Martine Jager, Takami Sato, Michael Zeschmick and the other, anonymous, reviewer(s) for their contribution to the peer review of this work. A peer review file is available.

Reprints and permissions information is available at <http://www.nature.com/reprints>

Publisher's note Springer Nature remains neutral with regard to jurisdictional claims in published maps and institutional affiliations.

Open Access This article is licensed under a Creative Commons Attribution-NonCommercial-NoDerivatives 4.0 International License, which permits any non-commercial use, sharing, distribution and reproduction in any medium or format, as long as you give appropriate credit to the original author(s) and the source, provide a link to the Creative Commons licence, and indicate if you modified the licensed material. You do not have permission under this licence to share adapted material derived from this article or parts of it. The images or other third party material in this article are included in the article's Creative Commons licence, unless indicated otherwise in a credit line to the material. If material is not included in the article's Creative Commons licence and your intended use is not permitted by statutory regulation or exceeds the permitted use, you will need to obtain permission directly from the copyright holder. To view a copy of this licence, visit <http://creativecommons.org/licenses/by-nc-nd/4.0/>.

© The Author(s) 2024